

Interplay between Adsorbates and Polarons: CO on Rutile TiO₂(110)Michele Retliccioli,¹ Igor Sokolović,² Michael Schmid,² Ulrike Diebold,² Martin Setvin,^{2,*} and Cesare Franchini^{1,3,†}¹University of Vienna, Faculty of Physics and Center for Computational Materials Science, Vienna 1090, Austria²Institute of Applied Physics, Technische Universität Wien, Vienna 1090, Austria³Dipartimento di Fisica e Astronomia, Università di Bologna, 40127 Bologna, Italy (Received 13 July 2018; revised manuscript received 26 November 2018; published 9 January 2019)

Polaron formation plays a major role in determining the structural, electrical, and chemical properties of ionic crystals. Using a combination of first-principles calculations, scanning tunneling microscopy, and atomic force microscopy, we analyze the interaction of polarons with CO molecules adsorbed on the reduced rutile TiO₂(110) surface. Adsorbed CO shows attractive coupling with polarons in the surface layer, and repulsive interaction with polarons in the subsurface layer. As a result, CO adsorption depends on the reduction state of the sample. For slightly reduced surfaces, many adsorption configurations with comparable adsorption energies exist and polarons reside in the subsurface layer. At strongly reduced surfaces, two adsorption configurations dominate: either inside an oxygen vacancy, or at surface Ti_{5c} sites, coupled with a surface polaron. Similar conclusions are predicted for TiO₂(110) surfaces containing near-surface Ti interstitials. These results show that polarons are of primary importance for understanding the performance of polar semiconductors and transition metal oxides in catalysis and energy-related applications.

DOI: [10.1103/PhysRevLett.122.016805](https://doi.org/10.1103/PhysRevLett.122.016805)

A wide range of materials form polaronic in-gap states upon injection of extra charge, as the excess electrons or holes couple to the lattice phonon field. The charge carriers generated by defects [1–6], doping [7–9], adsorbates [10–12], or irradiation [13–16], interact with the lattice field to different extents depending on the electron-phonon coupling, which is strongly material dependent [4,17,18]. The formation of polarons prevents a doping-driven insulator-to-metal transition and substantially alters the properties of the system and its functionalities [17,19,20]. In the strong short-range coupling limit, localized (so called small) polarons form; they locally distort the lattice and lead to the formation of in-gap states [21,22]. At low temperature, the ground state is determined by the polaronic configuration that minimizes the energy of the system [23,24], but even small thermal energies can activate polaron hopping to different hosting sites, thereby changing the nature and properties of the polaronic state [9,25–27].

The formation of polarons is particularly favorable in transition-metal oxides, owing to the strength of the electron-electron and electron-phonon interactions, and it is further promoted in the vicinity of the surface, where the crystal lattice is more flexible [27–30]. Therefore, polarons play a decisive role in physical and chemical phenomena taking place on oxide surfaces [27]. Here, we address the interactions between electron polarons and adsorbates. We show that adsorbates are able to alter the stability of polarons and, in turn, the polarons affect the energetics and configuration of the adsorbates. This interplay between adsorbates and polarons has direct impact on catalytic and energy conversion properties.

We considered CO molecules adsorbed on rutile titanium dioxide, an archetypal polaronic material [31]. In clean (i.e., without CO molecules) TiO₂(110) samples, the formation of polarons is promoted primarily by oxygen vacancies (V_O) and Ti interstitials (Ti_{int}) [11,32,33]. Oxygen vacancies are easily created at twofold-coordinated surface oxygen sites and each V_O donates two excess electrons that form polarons [34]; the polarons tend to reside at sixfold-coordinated Ti_{6c} atoms of the subsurface layer ($S1$) in the proximity of the V_O , due to the attractive polaron- V_O interaction [23,24,35–38]. Polaron hopping from $S1$ to the surface layer ($S0$) is unfavorable but may occur at elevated temperatures [4,8,24,26]. Interstitial Ti atoms, on the other hand, may occupy different lattice sites (difficult to detect in the experiments) and the four excess electrons associated to each Ti_{int} form more complicated polaron patterns, which have not been fully rationalized yet [39,40]. Our combined theoretical and (low temperature) experimental study is conducted on reduced samples containing V_O , in which the role of Ti_{int} is considered to be marginal, since the surface oxygen vacancies repel the positively charged Ti_{int} atoms, which are pushed deeper in the bulk [29].

The effect of polarons is usually not considered in adsorption studies. CO adsorption on the rutile (110) surface is a well-studied phenomenon, in particular for reduced surfaces containing V_O [39,41–47], yet controversies appear even in elementary issues. Beyond a general consensus on the local geometric properties (CO molecules adsorb vertically at fivefold-coordinated Ti_{5c} sites at low coverage) [41,42], conflicting outcomes have been reported, which

either suggest [43] or exclude [44–46] the possibility of CO adsorption at V_O sites. We show that the apparent disagreements in the literature can be resolved by a proper treatment of polarons and their interaction with adsorbates by combining density functional theory (DFT) simulations [48,49] with scanning tunneling microscopy (STM) and noncontact atomic force microscopy (nc-AFM). The strong-CO-polaron interaction substantially affects the adsorption energy and also the polaronic ground state.

We start by showing how the presence of CO alters the stability and orbital topology of polarons. We consider one CO molecule adsorbed at the Ti_{5c} site next nearest neighbor to the V_O (NNN- Ti_{5c}) for a V_O concentration of 5.6% (see Methods [50] for details). The spatial extension of the $S1$ and the $S0$ polaron electronic charge is shown in Figs. 1(a) and 1(b), respectively. The $S1$ polaron retains the same characteristic spatial distribution as in the absence of CO [24,63], with a d_{z^2} - $d_{x^2-y^2}$ -like orbital character at the hosting Ti_{6c} site and about 1/3 of the charge distributed on the surrounding atoms. Only very little (0.1%) polaronic charge is transferred to the CO molecule. This can be observed in filled-state STM images when the CO molecule is adsorbed above or in the proximity of an $S1$ polaron [see the weak circular spots in the inset of Fig. 1(a) and Fig. SF3 in the Supplemental Materials [50]].

Conversely, a polaron in the $S0$ layer strongly interacts with the CO molecule [Fig. 1(b)]. The $S0$ polaron acquires a stronger d_{yz} (54%) character as compared to the case with no adsorbates (43%) [24], and a non-negligible portion of the polaronic charge (1%) is transferred to the $2\pi^*$ antibonding orbital of the adsorbed CO [64,65]. This causes the formation of a double-lobed polaronic cloud above the CO molecule [see the filled-state STM images in the inset of Fig. 1(b)], which has a distinctly different shape from the one shown in Fig. 1(a) for a CO in the vicinity of an $S1$ polaron. The CO-polaron interaction affects strongly the polaron formation energies (E_{POL}), as shown in Fig. 1(c). While in the $S1$ case the polaron formation energy is

marginally destabilized by the CO ($\Delta E_{POL}^{S1} = +23$ meV), the formation of an $S0$ polaron becomes much more favorable ($\Delta E_{POL}^{S0} = -161$ meV): The adsorbate changes the polaronic ground state of the system, an effect that was overlooked in previous studies [39,66]. By inspecting the contributions to the polaron formation energy (determined by the balance between the electronic energy gain due to the electron-phonon coupling and the energy cost to locally distort the lattice [8]) we find that the presence of the CO reduces significantly the structural energy cost in the $S0$ polaron case. Moreover, we verified that CO adsorbed at a NNN- Ti_{5c} site with an $S0$ polaron below is more favorable than any other configuration (see Fig. SF5 [50]).

Next we focus on the CO adsorption as a function of the V_O concentration (c_{V_O}) and CO coverage (θ_{CO}), see Fig. 2. For locating the adsorbed CO we use nc-AFM imaging with a CO-terminated tip (blue-white images). The light (yellow)-black image show the polaron states mapped by filled-states STM images.

Figures 2(a) and 2(b) shows data obtained on a slightly reduced ($c_{V_O} = 5.8\%$) surface with a low CO coverage ($\theta_{CO} = 0.09$ ML). The CO molecules are predominantly adsorbed on Ti_{5c} sites [brighter spots in the AFM image in Fig. 2(a)], and less frequently at V_O sites (CO + V_O , solid circles). The filled-state STM image of the same region [Fig. 2(b)] shows mostly weak circular spots at the CO molecules on Ti_{5c} sites (two marked by down pointing triangles), which we attribute to the electronic cloud of $S1$ polarons in the vicinity of the CO, similar to those predicted in the inset of Fig. 1(a). There is only one intense double-lobed feature in the STM image [up pointing triangle in Fig. 2(b)], sandwiched by two oxygen vacancies (see also Fig. SF6 [50]). We attribute this to a CO at the NNN- Ti_{5c} site, coupled to an $S0$ polaron (CO + $S0$ -polaron complex), as predicted in Fig. 1(b). The CO adsorbed at V_O sites (solid circles in Fig. 2) observed by nc-AFM is invisible in filled-state STM images, since the polaronic clouds do not extend to these sites and these molecules have no in-gap states.

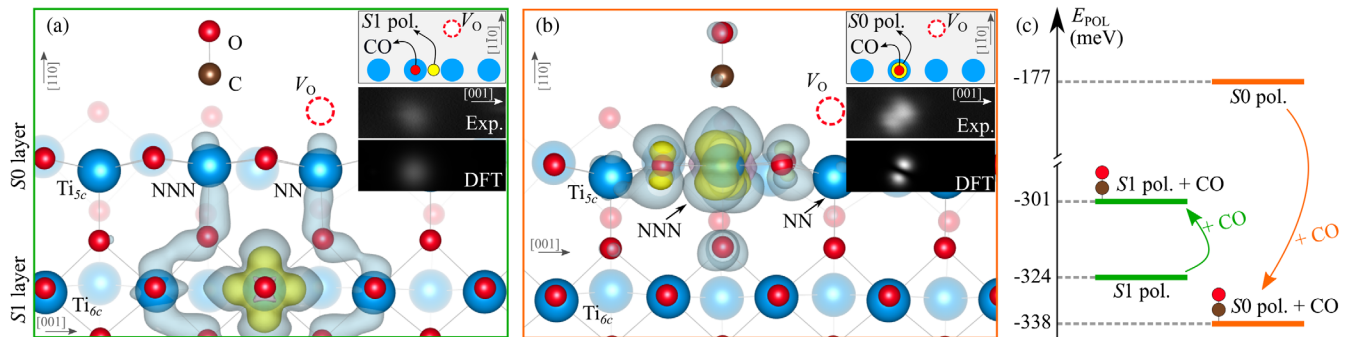


FIG. 1. Effects of a CO molecule adsorbed at NNN- Ti_{5c} site on polaronic states at low reduction level (5.6%, i.e., one V_O in a 9×2 two-dimensional unit cell). (a) and (b) electronic charge density of the $S1$ (a) and $S0$ (b) polarons in presence of CO. Atoms at the back are depicted by bleached spheres. A top view of the considered configuration is also sketched in each panel. The insets represent the experimental and simulated filled-state STM images. (c) Polaron formation energy of $S0$ and $S1$ polarons, in case of a $TiO_2(110)$ surface with and without adsorbed CO.

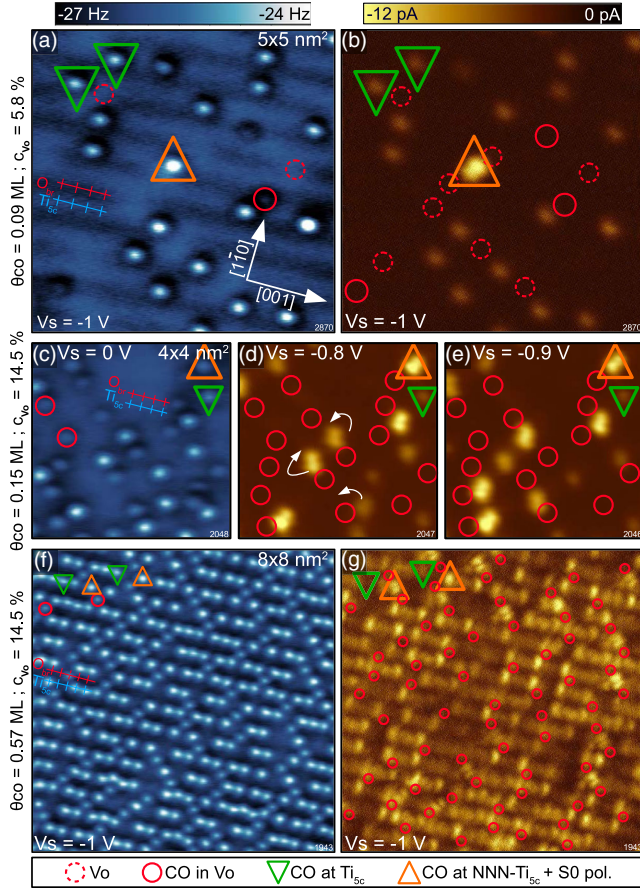


FIG. 2. Experimental constant-height nc-AFM (blue-white) and filled-state STM images (yellow-black) of CO adsorbed on the rutile (110) surfaces at different surface reduction states. Dashed circles show the positions of V_O s, solid circles show V_O s with an adsorbed CO molecule, triangles show CO molecules adsorbed on Ti_{5c} atoms. Down-pointing triangles indicate coupling with $S1$ polarons, up-pointing triangles indicate coupling with $S0$ polarons. (a) and (b) Low CO coverage and low reduction level ($\theta_{CO} = 0.09$ ML and $c_{V_O} = 5.8\%$). (c), (d), and (e) moderate CO coverage and high reduction level ($\theta_{CO} = 0.15$ ML and $c_{V_O} = 14.5\%$). The STM images (d) and (e) were measured sequentially, and the arrows indicate the diffusion of CO along Ti_{5c} sites, accompanied by polaron hopping. (f) and (g) High CO coverage and high reduction level ($\theta_{CO} = 0.57$ ML and $c_{V_O} = 14.5\%$).

At a more reduced surface ($c_{V_O} = 14.5\%$ and $\theta_{CO} = 0.15$ ML), the nc-AFM image shows that all V_O sites are occupied by CO molecules [Fig. 2(c)]. The filled-states STM images of the same region show many double-lobed CO molecules at Ti_{5c} sites, indicating the formation of CO + $S0$ -polaron complexes [Figs. 2(d) and 2(e)]. The two consecutive filled-state STM images Figs. 2(d) and 2(e) show diffusion of several CO molecules. The molecules become brighter or darker when they move closer or further away from the V_O s, respectively. We attribute these changes to their coupling to $S0$ and $S1$ polarons.

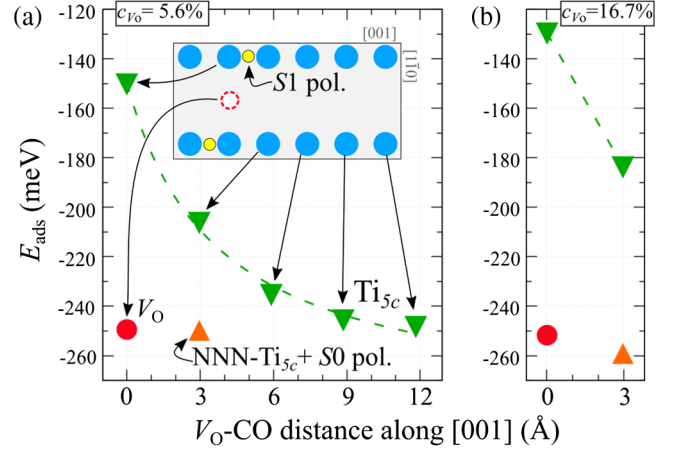


FIG. 3. Site-dependent adsorption energy. A CO molecule explores Ti_{5c} sites at various distances from the oxygen vacancy (down pointing triangles), and the V_O site (circle), in the presence of polarons localized at the $S1$ layer in a reduced slab with $c_{V_O} = 5.6\%$ (a) and $c_{V_O} = 16.7\%$ (b). The inset sketches the considered configurations. In addition, we report the case of adsorption at the NNN- Ti_{5c} hosting an $S0$ polaron (up pointing triangle).

Finally, by further increasing the CO concentration up to $\theta_{CO} = 0.57$ ML [67] at the highly reduced surface ($c_{V_O} = 14.5\%$), all oxygen vacancies are occupied by CO molecules [Fig. 2(f)], again with no in-gap state found there in the filled-state STM images [Fig. 2(g)]. The nc-AFM image clearly shows that CO avoids V_O -nearest-neighbor sites [Fig. 2(f)], and prefers NNN- Ti_{5c} sites in combination with the $S0$ polaron [double-lobed features in Fig. 2(g), particularly intense when the CO is adsorbed at a NNN- Ti_{5c} site sandwiched between two V_O s]. CO molecules adsorb also at other Ti_{5c} sites, characterized by weaker STM signals. These weak filled states originate from “tails” of electronic charges of $S1$ polarons and of CO + $S0$ -polaron complexes spreading over CO molecules at neighboring Ti_{5c} sites (see Fig. SF4 [50]). We note that all filled states measured on the CO molecules are deep in-gap states; i.e., no tunneling current is measured for small sample biases ($V_S > -0.6$ V): this confirms the polaronic character of these electronic states.

The interpretation of the experimental data is supported by calculated site-dependent CO adsorption energies (E_{ads}), see Fig. 3. At low reduction [$c_{V_O} = 5.6\%$, Fig. 3(a)], the stability of the CO adsorption at nonpolaronic Ti_{5c} sites (i.e., CO + $S1$ configurations, down pointing triangles) increases with an increasing distance from the V_O , in accordance with the experiment [see CO + $S1$ circular spots in Fig. 2(b)]. CO adsorption at a V_O (CO + V_O) or at polaronic NNN- Ti_{5c} (CO + $S0$ -polaron complex) sites are essentially degenerate in energy, comparable to the most favorable CO + $S1$ -polaron configurations. In the experiment, the rare occurrence of the double-lobed CO + $S0$ spots and CO + V_O features [Figs. 2(a) and 2(b)] originates from a smaller number of available NNN- Ti_{5c} and V_O

adsorption sites, as compared to the nonpolaronic Ti_{5c} sites [43].

For a strongly reduced surface [$c_{V_O} = 16.7\%$, Fig. 3(b)], adsorption at Ti_{5c} sites in combination with $S1$ polarons becomes less favorable, mainly due to the absence of Ti_{5c} sites at large distances from the V_O s, whereas the $\text{CO} + S0$ -polaron and $\text{CO} + V_O$ configurations retain their high stability and represent the most stable solutions. This is in excellent agreement with the filled-state STM measurements showing an increase of double-lobed spots arising from $\text{CO} + S0$ -polaron complexes with increasing c_{V_O} [see Figs. 2(c)–2(g)] combined with a large density of $\text{CO} + V_O$ features [see Figs. 2(c) and 2(f)]. The formation of the $\text{CO} + S0$ -polaron complexes on the strongly reduced sample is in line with the previously reported polaron dynamics on clean surfaces [27]: In strongly reduced TiO_2 , the $S1$ -to- $S0$ polaron hopping is promoted by the repulsive polaron-polaron interactions in the $S1$ layer and by the attraction of polarons to the V_O 's (see Fig. SF1) [24].

The interaction between polarons and adsorbed CO molecules significantly affects the adsorption energies (Fig. SF7 [50]), the bonding distances from the surface as well as the CO bond length (Fig. SF2 [50]). The various polaron- CO coupling schemes reported here are consistent with reported experimental data on CO adsorption: Temperature-programmed desorption shows multiple desorption peaks on the rutile (110) surface [47]. In contrast, the same experiment performed on the anatase $\text{TiO}_2(101)$ surface [68] shows a single peak only. This can be associated with the absence of small polarons at the anatase (101) surface [4], which simplifies the adsorption in comparison to the polaronic rutile. Similarly, infrared absorption spectra of CO on the anatase (101) surface always exhibit a single C-O vibrational peak [68], while the rutile (110) surface shows either one or two peaks, depending on the reduction level of the crystal [45]. We identify the additional vibrational frequency as CO coupled with the $S0$ surface polaron and to CO adsorbed at oxygen vacancies (see Fig. SF8 [50]).

For the sake of completeness and to underline the generality of our conclusions, we inspected by DFT also the CO adsorption under the influence of polarons caused by Ti_{int} s (see Fig. SF9 [50]). In the absence of nearby V_O the Ti_{int} -induced excess electrons lead to the formation of robust $\text{CO} + S0$ -polaron complexes, which exhibit the characteristic double-lobed feature in the simulated STM images, in analogy with the V_O case (see Fig. SF10 [50]). Our experiments on V_O -reduced samples detect the double-lobed STM signal only in correlation with the V_O (precisely, on NNN-Ti_{5c} sites). This is an additional indication that near-surface Ti_{int} s are not present in samples with V_O s.

In summary, by combining first-principles calculations and surface-sensitive techniques we have elucidated the key role of the interaction between polarons and CO adsorbates on V_O -reduced rutile $\text{TiO}_2(110)$. We have shown that CO

adsorption promotes polaron transfer from subsurface to surface sites, in particular at highly reduced TiO_2 samples, enhancing the activity of surface Ti_{5c} sites. We have identified three distinct adsorption configurations: CO at V_O sites, CO at Ti_{5c} sites weakly coupled with polarons in the subsurface (manifested by weak circular features in filled-state STM), and strongly coupled $\text{CO} + S0$ -polaron complexes at NNN-Ti_{5c} sites (appearing as double-lobes in filled-state STM). The coupling between CO and polarons and its interaction with V_O s strongly influences CO adsorption and causes breaking and recombination of the $\text{CO} + S0/S1$ complexes. Similar conclusions are valid for the Ti_{int} -reduced surfaces, since shallow Ti_{int} atoms promote the formation of $S0$ polarons and, consequently, of $\text{CO} + S0$ -polaron complexes on V_O -free surfaces. Our study delivers a consistent and comprehensive picture of CO adsorption on an archetypal polaronic material, solves long-standing ambiguities and conflicting interpretations of experimental results, and sets the path for revisiting the interpretation of adsorption processes in polar semiconductors and transition metal oxides.

This work was supported by the Austrian Science Fund (FWF) Projects No. ViCoM (F4109) and No. POLOX (I 2460), Doctoraal College “Solids4Fun” (W 1234), and Wittgenstein-prize (Z250-N16), by the ERC Advanced Research Grant “OxideSurfaces,” and by the Ph.D. Completion Fellowship of the University of Vienna. The computational results were achieved by using the Vienna Scientific Cluster (VSC).

*setvin@iap.tuwien.ac.at

†cesare.franchini@univie.ac.at

- [1] E. Finazzi, C. D. Valentin, G. Pacchioni, C. Di Valentin, and G. Pacchioni, *J. Phys. Chem. C* **113**, 3382 (2009).
- [2] X. Mao, X. Lang, Z. Wang, Q. Hao, B. Wen, Z. Ren, D. Dai, C. Zhou, L.-M. Liu, and X. Yang, *J. Phys. Chem. Lett.* **4**, 3839 (2013).
- [3] S. Moser, L. Moreschini, J. Jaćimović, O. S. Barišić, H. Berger, A. Magrez, Y. J. Chang, K. S. Kim, A. Bostwick, E. Rotenberg, L. Forró, and M. Grioni, *Phys. Rev. Lett.* **110**, 196403 (2013).
- [4] M. Setvin, C. Franchini, X. Hao, M. Schmid, A. Janotti, M. Kaltak, C. G. Van De Walle, G. Kresse, and U. Diebold, *Phys. Rev. Lett.* **113**, 086402 (2014).
- [5] P. Deák, J. Kullgren, and T. Frauenheim, *Phys. Status Solidi RRL* **8**, 583 (2014).
- [6] C. Verdi, F. Caruso, and F. Giustino, *Nat. Commun.* **8**, 15769 (2017).
- [7] C. Crevecoeur and H. De Wit, *J. Phys. Chem. Solids* **31**, 783 (1970).
- [8] A. Janotti, C. Franchini, J. B. Varley, G. Kresse, and C. G. Van de Walle, *Phys. Status Solidi RRL* **7**, 199 (2013).
- [9] X. Hao, Z. Wang, M. Schmid, U. Diebold, and C. Franchini, *Phys. Rev. B* **91**, 085204 (2015).
- [10] C. Di Valentin, G. Pacchioni, and A. Selloni, *Phys. Rev. Lett.* **97**, 166803 (2006).

- [11] N. A. Deskins, R. Rousseau, and M. Dupuis, *J. Phys. Chem. C* **113**, 14583 (2009).
- [12] H. Sezen, M. Buchholz, A. Nefedov, C. Natzeck, S. Heissler, C. Di Valentin, and C. Wöll, *Sci. Rep.* **4**, 3808 (2015).
- [13] H. Sezen, H. Shang, F. Bebensee, C. Yang, M. Buchholz, A. Nefedov, S. Heissler, C. Carbogno, M. Scheffler, P. Rinke, and C. Wöll, *Nat. Commun.* **6**, 6901 (2015).
- [14] F. Freytag, G. Corradi, and M. Imlau, *Sci. Rep.* **6**, 36929 (2016).
- [15] L. M. Carneiro, S. K. Cushing, C. Liu, Y. Su, P. Yang, A. P. Alivisatos, and S. R. Leone, *Nat. Mater.* **16**, 819 (2017).
- [16] K. Miyata, D. Meggiolaro, M. T. Trinh, P. P. Joshi, E. Mosconi, S. C. Jones, F. De Angelis, and X.-Y. Zhu, *Sci. Adv.* **3**, e1701217 (2017).
- [17] A. S. Alexandrov and J. T. Devreese, *Advances in Polaron Physics*, Springer Series in Solid-State Sciences (Springer-Verlag, Berlin, 2010).
- [18] F. Giustino, *Rev. Mod. Phys.* **89**, 015003 (2017).
- [19] I. G. Austin and N. F. Mott, *Adv. Phys.* **50**, 757 (2001).
- [20] A. M. Stoneham, J. Gavartin, A. L. Shluger, A. V. Kimmel, D. M. Ramo, H. M. Rønnow, G. Aeppli, and C. Renner, *J. Phys. Condens. Matter* **19**, 255208 (2007).
- [21] A. M. Stoneham, *J. Chem. Soc., Faraday Trans. 2* **85**, 505 (1989).
- [22] A. L. Shluger and A. M. Stoneham, *J. Phys. Condens. Matter* **5**, 3049 (1993).
- [23] N. A. Deskins, R. Rousseau, and M. Dupuis, *J. Phys. Chem. C* **115**, 7562 (2011).
- [24] M. Reticcioli, M. Setvin, M. Schmid, U. Diebold, and C. Franchini, *Phys. Rev. B* **98**, 045306 (2018).
- [25] Z. Dohnálek, I. Lyubnitsky, and R. Rousseau, *Prog. Surf. Sci.* **85**, 161 (2010).
- [26] P. M. Kowalski, M. F. Camellone, N. N. Nair, B. Meyer, and D. Marx, *Phys. Rev. Lett.* **105**, 146405 (2010).
- [27] M. Reticcioli, M. Setvin, X. Hao, P. Flauger, G. Kresse, M. Schmid, U. Diebold, and C. Franchini, *Phys. Rev. X* **7**, 031053 (2017).
- [28] P. Krüger, S. Bourgeois, B. Domenichini, H. Magnan, D. Chandesris, P. Le Fèvre, A. M. Flank, J. Jupille, L. Floreano, A. Cossaro, A. Verdini, and A. Morgante, *Phys. Rev. Lett.* **100**, 055501 (2008).
- [29] Y. Yoon, Y. Du, J. C. Garcia, Z. Zhu, Z.-T. Wang, N. G. Petrik, G. A. Kimmel, Z. Dohnalek, M. A. Henderson, R. Rousseau, N. A. Deskins, and I. Lyubnitsky, *Chem. Phys. Chem.* **16**, 313 (2015).
- [30] T. Shibuya, K. Yasuoka, S. Mirbt, and B. Sanyal, *J. Phys. Chem. C* **121**, 11325 (2017).
- [31] V. N. Bogomolov and D. N. Mirlin, *Phys. Status Solidi B* **27**, 443 (1968).
- [32] S. Wendt, P. T. Sprunger, E. Lira, G. K. H. Madsen, Z. Li, J. Ø. Hansen, J. Matthiesen, A. Blekinge-Rasmussen, E. Lægsgaard, B. Hammer, and F. Besenbacher, *Science* **320**, 1755 (2008).
- [33] A. C. Papageorgiou, N. S. Beglitis, C. L. Pang, G. Teobaldi, G. Cabailh, Q. Chen, A. J. Fisher, W. A. Hofer, and G. Thornton, *Proc. Natl. Acad. Sci. U.S.A.* **107**, 2391 (2010).
- [34] P. G. Moses, A. Janotti, C. Franchini, G. Kresse, and C. G. Van De Walle, *J. Appl. Phys.* **119**, 181503 (2016).
- [35] U. Diebold, S.-c. Li, and M. Schmid, *Annu. Rev. Phys. Chem.* **61**, 129 (2010).
- [36] M. A. Henderson, *Surf. Sci. Rep.* **66**, 185 (2011).
- [37] T. Shibuya, K. Yasuoka, S. Mirbt, and B. Sanyal, *J. Phys. Chem. C* **118**, 9429 (2014).
- [38] C. M. Yim, M. B. Watkins, M. J. Wolf, C. L. Pang, K. Hermansson, and G. Thornton, *Phys. Rev. Lett.* **117**, 116402 (2016).
- [39] Y.-Y. Yu and X.-Q. Gong, *ACS Catal.* **5**, 2042 (2015).
- [40] K. Morita, T. Shibuya, and K. Yasuoka, *J. Phys. Chem. C* **121**, 1602 (2017).
- [41] U. Diebold, *Surf. Sci. Rep.* **48**, 53 (2003).
- [42] J. P. Prates Ramalho, F. Illas, and J. R. B. Gomes, *Phys. Chem. Chem. Phys.* **19**, 2487 (2017).
- [43] R. Mu, A. Dahal, Z.-T. Wang, Z. Dohnálek, G. A. Kimmel, N. G. Petrik, and I. Lyubnitsky, *J. Phys. Chem. Lett.* **8**, 4565 (2017).
- [44] Y. Zhao, Z. Wang, X. Cui, T. Huang, B. Wang, Y. Luo, J. Yang, and J. Hou, *J. Am. Chem. Soc.* **131**, 7958 (2009).
- [45] M. Xu, H. Noei, K. Fink, M. Muhler, Y. Wang, and C. Wöll, *Angew. Chem., Int. Ed.* **51**, 4731 (2012).
- [46] Y. Cao, M. Yu, S. Qi, S. Huang, T. Wang, M. Xu, S. Hu, and S. Yan, *Sci. Rep.* **7**, 6148 (2017).
- [47] N. G. Petrik and G. A. Kimmel, *J. Phys. Chem. Lett.* **3**, 3425 (2012).
- [48] G. Kresse and J. Furthmüller, *Phys. Rev. B* **54**, 11169 (1996).
- [49] G. Kresse and J. Furthmüller, *Comput. Mater. Sci.* **6**, 15 (1996).
- [50] See Supplemental Material at <http://link.aps.org/supplemental/10.1103/PhysRevLett.122.016805> for further details, which includes Refs. [51–62].
- [51] J. P. Perdew, K. Burke, and M. Ernzerhof, *Phys. Rev. Lett.* **77**, 3865 (1996).
- [52] J. Klimeš, D. R. Bowler, and A. Michaelides, *J. Phys. Condens. Matter* **22**, 022201 (2010).
- [53] M. Dion, H. Rydberg, E. Schröder, D. C. Langreth, and B. I. Lundqvist, *Phys. Rev. Lett.* **92**, 246401 (2004).
- [54] Z. Wang, C. Brock, A. Matt, and K. H. Bevan, *Phys. Rev. B* **96**, 125150 (2017).
- [55] S. L. Dudarev, G. A. Botton, S. Y. Savrasov, C. J. Humphreys, and A. P. Sutton, *Phys. Rev. B* **57**, 1505 (1998).
- [56] F. J. Giessibl, U.S. Patent No. 2012/0131704 A1 (2012).
- [57] F. Huber and F. J. Giessibl, *Rev. Sci. Instrum.* **88**, 073702 (2017).
- [58] M. Setvín, J. Javorský, D. Turčínková, I. Matolínová, P. Sobotík, P. Kocán, and I. Ošťádal, *Ultramicroscopy* **113**, 152 (2012).
- [59] L. Sun, X. Huang, L. Wang, and A. Janotti, *Phys. Rev. B* **95**, 245101 (2017).
- [60] S. Grimme, J. Antony, S. Ehrlich, and H. Krieg, *J. Chem. Phys.* **132**, 154104 (2010).
- [61] S. Grimme, S. Ehrlich, and L. Goerigk, *J. Comput. Chem.* **32**, 1456 (2011).
- [62] B. Wen, W.-J. Yin, A. Selloni, and L.-M. Liu, *J. Phys. Chem. Lett.* **9**, 5281 (2018).

- [63] T. Shibuya, K. Yasuoka, S. Mirbt, and B. Sanyal, *J. Phys. Condens. Matter* **24**, 435504 (2012).
- [64] P. S. Bagus, C. J. Nelin, and C. W. Bauschlicher, *Phys. Rev. B* **28**, 5423 (1983).
- [65] K. I. Hadjiivanov and G. N. Vayssilov, *Adv. Catal.* **47**, 307 (2002).
- [66] M. Farnesi Camellone, P. M. Kowalski, and D. Marx, *Phys. Rev. B* **84**, 035413 (2011).
- [67] The high coverage was determined by counting the total number of Ti_{5c} sites (415) and vacancies (14.5%) occupied by CO.
- [68] M. Setvin, M. Buchholz, W. Hou, C. Zhang, B. Stöger, J. Hulva, T. Simschitz, X. Shi, J. Pavelec, G. S. Parkinson, M. Xu, Y. Wang, M. Schmid, C. Wöll, A. Selloni, and U. Diebold, *J. Phys. Chem. C* **119**, 21044 (2015).